KSME International Journal, Vol. 13, No. 10, pp. 701~713, 1999

Sculptured Surface Recognition and Localization Strategy in the CMM Process

Myeong-Woo Cho* and Tae-Il Seo**

(Received January 11, 1999)

This paper presents a sculptured surface recognition and localization strategy for the inspection process using the CMM. First, the database is generated from the CAD data based on the Z-Layer concept. Then, the three-dimensional shape of the object on the CMM table is constructed using a vision guided CMM. Two vision cameras are implemented to guide the CMM to the object, and B-spline interpolation method is applied to generate a surface that passes through the obtained data points. As a following step, the Z-layers of the generated surface are created and the geometric properties are calculated to determine the best matching surface in the database. Rough location and orientation of the object are determined by analyzing the image data, and the minimization algorithm is applied as a next step to obtain more accurate localization results. The experimental results show that the proposed method can be applied effectively for sculptured surface recognition and localization in the inspection processes.

Key Words: Coordinate Measuring Machine, Sculptured Surface, Recognition, Localization

1. Introduction

The three-dimensional Coordinate Measuring Machine (CMM) plays an increasingly important role as a measuring station for precise and complicated workpiece shapes such as sculptured surfaces. The sculptured surfaces are found in various products such as automobile bodies, mold cavities, stamping dies and turbine blades. However, the current manufacturing styles are being rapidly changed into small-batch and flexible manufacturing systems. Since, in general, only sampled workpieces are measured in the manufacturing process, the objects to be inspected using CMM will be changed more frequently. If the inspection process must deal with frequently changing objects, the inspection process will become a very tedious job. Thus, the development of suitable object recognition and localization methods is indispensable to make the CMM a truly flexible automated inspection system.

For the recognition of a curved object, Sato and Honda (1983) proposed a pseudo distance measuring method. They considered the curved object as an accumulation of horizontal section boundaries. Wang et al. (1984) proposed a three-dimensional object matching method using the silhouettes. They identified the objects by calculating the moment invariants from the front, side, and top silhouettes of an object. Lo and Don (1989) proposed an object identification method using three-dimensional moments. Liu and Tsai (1990) proposed a method for the curved object recognition using multiple camera views. They tried to recognize the object by taking a top view and several side views of an object placed on a rotating table.

In this study, a sculptured surface recognition/localization method is proposed by integrating the vision system and the CMM. The schematic diagram of the proposed object recognition and localization method is shown in Fig. 1. As shown

* Assistant Professor, School of Mechanical/Aerospace/Automation Engineering, Inha University, Inchon, Korea

** Research Fellow, Research Institute for Mechanical Engineering, Inha University, Inchon, Korea

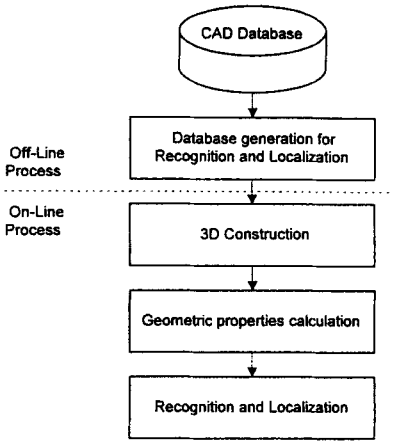

Fig. 1 Overall schematic diagram for the proposed method.

in the figure, the recognition/localization database is generated from the CAD data. Then, the three-dimensional shape of the object on the CMM table is constructed using the proposed method. In the proposed system, two vision cameras are used to guide the CMM to the object. Then, surface interpolation method is applied to generate a surface that passes through all the measured data points by the CMM. As a following step, the Z-layers of the generated surface are created, and the geometric properties of each layer are calculated. These results are used to determine the best matching surface in the generated database. Rough location and orientation of the object are determined using the image data and, as a next step, the minimization algorithm is applied to obtain more accurate localization results. Finally, several experiments are performed to show the effectiveness of the proposed sculptured surface recognition and localization method.

2. Database Construction Based on Z-Layer Concept

As shown in Fig. 2, the Z-layers are defined as several cross-sections that are parallel to the xy-plane (Cho et al., 1995). To generate the required database, first, a surface is represented as the Z-map that is an array of the z-coordinates of a surface (Takeuchi et al., 1990). Then, the Z-map

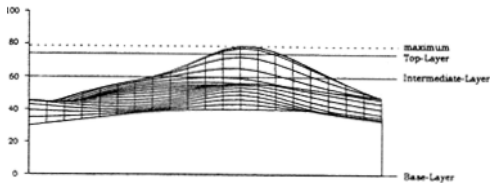

Fig. 2 Definition of the Z-layers.

is cut at several heights, and the cross-sections of the surface are considered as binary images. The required recognition/localization database can be constructed by calculating the geometric properties of each layer.

2.1 Creation of the Z-layers

The Z-layer is an array whose element value is either 0 or 1. This value can be obtained from the Z-map by slicing the object at certain heights. If the z-value of an element is greater than the pre-defined value, then the Z-layer element has a value of 1, otherwise it has a value of 0. Then, each Z-layer will have a similar shape to the binary image, and the size of the Z-layer array is the same as that of the Z-map. By applying the binary image processing techniques, the geometric properties (such as area, centroid, moment of inertia, etc.) can be obtained from the Z-layer. Since each surface has different geometric properties, the sculptured surface can be identified by a set of Z-layers.

To create the Z-layers, the maximum height of the surface is first obtained, and it is divided into certain levels according to the pre-defined height ratios. In this study, three Z-layers, denoted by Base-Layer, Top-Layer and Intermediate-Layer, are created to identify each surface as shown in Fig. 3. The height ratios for each layer are set to 0.0, 0.9, 0.7, respectively.

Among the layers, the base-layer has the most important information. Since the height ratio is set to 0, this layer can be regarded as a projected image of an object onto the xy-plane. The basic characteristics obtained from this layer can be used for recognition and rough localization of the object. The next significant layer is the top-layer. The height ratio to create this layer is set to 0.9 since the geometric features of the higher regions

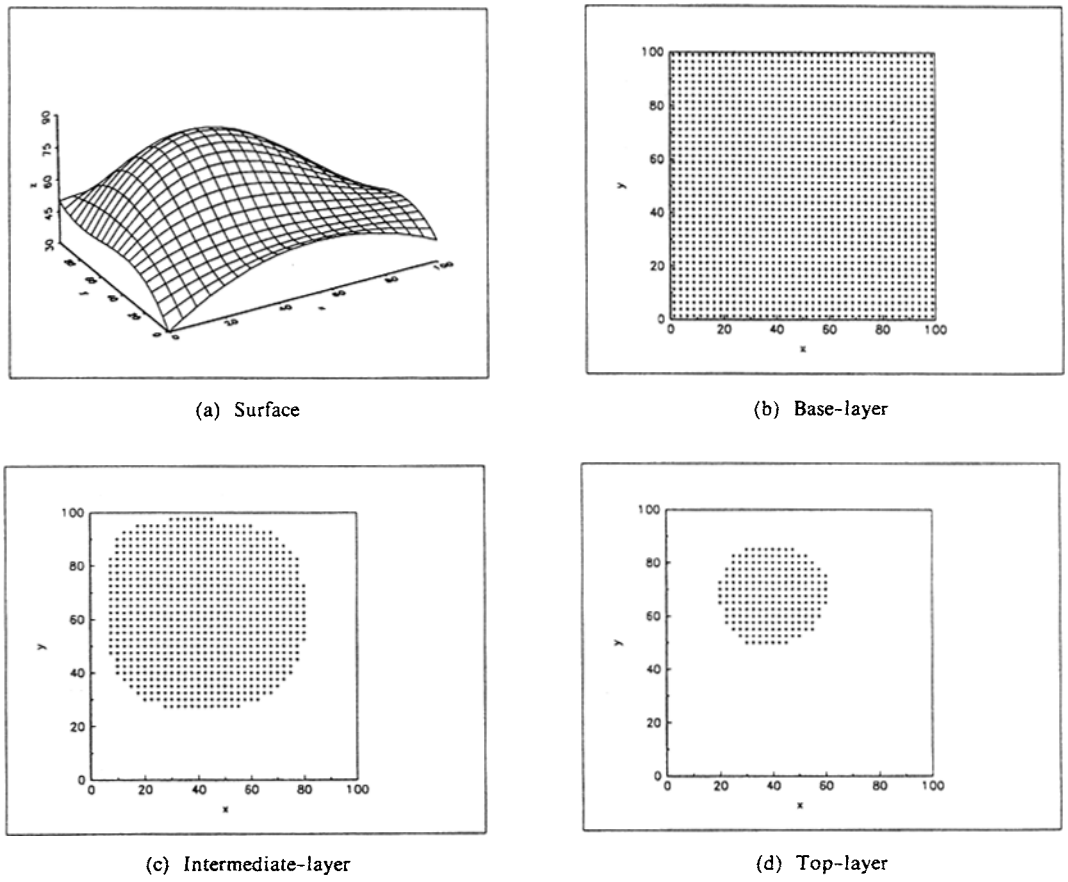

Fig. 3 Z-Layers of a surface.

around the maximum-height point are required. Thus, the results can also be used as effective criteria for surface recognition and localization. In many cases, the sculptured surface can be identified by analyzing the base-layer and top-layer since the most significant information can be extracted from these two layers. The number of Z-layers can be increased when the difficulty of surface identification increases. If there are many objects in a set to be inspected, and if the surface shapes are similar to each other, then the number of Z-layers must be increased appropriately to identify all the objects in a set. Thus, in this study, one more layer (intermediate layer) is created to obtain more accurate recognition and localization results. The height ratios used to create the top-layer and intermediate-layer can be changed to obtain more satisfactory results, however, the ratios should be kept constant for a set of objects to be recognized.

2.2 Geometric properties of the Z-layers

As previously discussed, since the Z-layer elements have a value of either 1 or 0, each Z-layer can be represented as a binary image that contains black and white pixels. Here, the elements having a value of 1 will be assigned to white pixels (the projected part of the object), and the others will be assigned to black pixels (the blank part of the binary image). Each Z-layer can be regarded as a projected image of an object that has the same geometric properties. Therefore, general binary image processing techniques can be applied to calculate the geometric properties of the Z-layers.

In this study, four specific properties are used for each layer to recognize a set of surfaces: area of the projected image, centroid of the area, moment of inertia around the centroid, and eccen-

Table 1 Geometric features for each layer.

Features	Base-Layer (F_B)	Others (F_T, F_m)
F_1	Area of image	Area of the image
F_2	Maximum height of the surface	Height of the layer
F_3	Moment of inertia around the centroid	Moment of inertia around the centroid
F_4	Eccentricity	Eccentricity
F_5	x-coordinate of the centroid in the workpiece coordinate	Number of regions
F_6	y-coordinate of the centroid in the workpiece coordinate	Distance between the centroids of base and other layer
F_7	—	Inclination of the line connecting the centroids of base and other layer

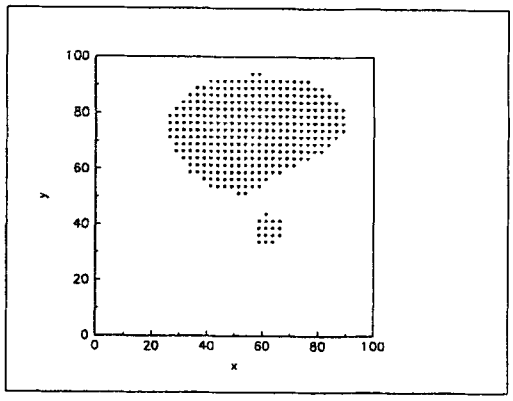

Fig. 4 An example of a Z-layer having two separate regions.

tricity of the images. Among the properties, the centroid has two values, i. e., x- and y-coordinates, and the other properties have one value. For the base-layer, the x- and y-coordinates of the centroid are calculated. The distance between the two centroids (base-layer and the other layer' s centroids) is calculated for other layers. Besides these properties, the maximum height of the surface is included in the features of the base-layer, and the height of each layer is added to the features of each layer. Also, the number of separate regions in each layer and the relative angle of the layer must be known for the top and intermediate layers because it is possible to have more than one region in a layer as shown in Fig. 4. In this case, first, the sequential labeling algorithm (Horn, 1986) should be applied to label the separate regions of the Z-layer, and next, the geometric properties should be calculated for each separate region. Thus, a total of six types of features are used for the base-layer, and seven types of features are used for the other layers for the recognition and localization of the objects. The required features for each layer are listed in Table 1. Here, the moment of inertia around the centroid and the eccentricity are called the *first* and *second moment invariants* respectively, which are invariant features for translation and rotation (Wang et. al., 1984). Calculation methods for the geometric properties are shown in the Appendix.

3. Surface Construction of the Object

In this study, two vision cameras and CMM are integrated to recognize the object placed on the CMM table. To obtain more desired results from the sparse data set, B-spline interpolation method is applied to generate the surface information, and the geometric properties are calculated to determine the best matching surface. The proposed surface construction procedures are as described below.

3.1 Proposed system

The proposed system uses the CMM and two cameras as shown in Fig. 5. One camera is

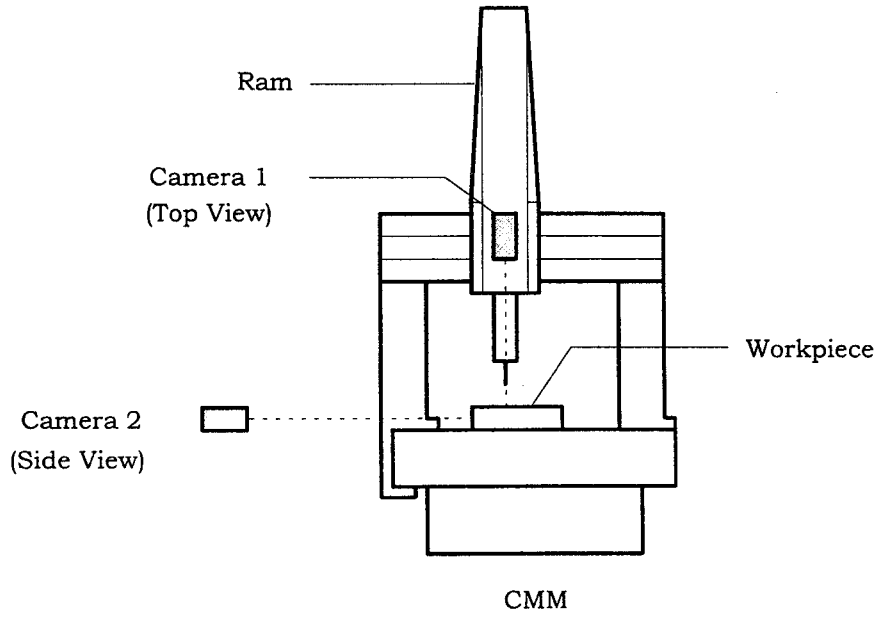

Fig. 5 Proposed system.

mounted on the ram of the CMM to take the top-view of the object. Using the binary image processing techniques, this top-view image is analyzed to determine the area, position, orientation, and the size of the object. The other camera is placed at the side of the CMM to take the side-view of the object. The height of the object can be determined from this image. The proposed algorithm to construct three-dimensional data of the given surface is as follows:

Step1 : Top-view analysis.

1. Take the top-view.
2. Calculate the position, orientation, area, and the size of the object from the top-view.
3. Determine the optimum step size for digitization that is based on the length along the principal axis of the object.
4. Transform the probe contact points array according to the position and orientation of the object.

Step 2 : Side-view analysis.

1. Take the side-view.
2. Determine the maximum height of the object from the side-view.
3. Calculate the guide point locations.

Step 3 : Surface construction.

1. Digitize the surface in a rectangular array form.
2. Generate the surface using B-spline interpolation.

The digitizing area must be slightly smaller than the base size of the surface to avoid digitizing failure. After deciding the optimum step size, the array of measuring points is transformed according to the position and orientation of the principal axis that can be obtained from the top-view image.

3.2 Surface generation using interpolation method

An efficient algorithm to generate a B-spline interpolation surface is proposed by Wang et al. (1990). Their method is based on the B-spline approximation and finds new control vertices that can make the surface pass through all the given data points using numerical methods. Therefore, the number of control vertices will be the same as the number of data points. The recursive equation of the B-spline surface can be given as

$$\vec{s}(u, v) = \sum_{i=0}^{m} \sum_{j=0}^{n} \vec{p}_{i,j} \cdot N_i(u) M_j(v) \qquad (1)$$

where $p_{i,j}$ are the vertices of the control polyhedron, $N_i(u)$ and $M_j(v)$ are the B-spline basis functions in the u and v direction on the surface. In order to obtain the surface which passes through a data set given by $d_{i,j}$ the following set of linear equations should be solved for each knot value u_i and v_j.

$$d_{i,j}=\tilde{s}(u_i, v_j)=\sum_{k=0}^{m}\sum_{l=0}^{n}\tilde{p}_{k,l}\cdot N_k(u_i)M_l(v_j) \quad (2)$$

where m and n denote the size of the data points.

Since B-splines have local support, for the case of the fourth order B-splines, the above equation can be rewritten as follows (Wang et al., 1990):

$$\begin{aligned} d_{i,j}=\frac{1}{36}[&(p_{i-1,j-1}+4p_{i,j-1}+p_{i+1,j-1})\\ &+4(p_{i-1,j}+4p_{i,j}+p_{i+1,j})\\ &+(p_{i-1,j+1}+4p_{i,j+1}+p_{i+1,j+1})] \end{aligned} \quad (3)$$

Therefore, to solve the B-spline interpolation problem, the following recursive equation should be solved.

$$\begin{aligned} &p_{i,j}^{k+1}=p_{i,j}^{k}+(d_{i,j}-B_{i,j}), \text{ for } k\geq 0 \text{ with}\\ &p_{i,j}^{0}=d_{i,j} \end{aligned} \quad (4)$$

where, $B_{i,j}$ denotes the right hand side of Eq. (3). Then, $(d_{i,j}-B_{i,j})$ can be regarded as the error in the k^{th} iteration based on the control coefficients $p_{i,j}^{k}$. The iteration process will be continued until the error is sufficiently small for the application.

4. Matching

After calculating all the required geometric properties for the surface to be inspected, it is essential to match the surface with the given database. As a first step, the base-layer will be investigated because it contains the most important information. Next, the features of the other layers will be analyzed until the given object can be recognized. Among the properties of the base-layer, $(F_{B1})_R-(F_{B4})_R$ will be used to recognize the surface and the other features ($(F_{B5})_R$, $(F_{B6})_R$) will be used to determine the location of the surface. The first possible set of surfaces can be determined by calculating the following mismatch measure values for the base-layer.

Let $F_R=\{(F_{B1})_R\ (F_{B2})_R\ (F_{B3})_R\ (F_{B4})_R\}$, for the calculated base-layer features, and $F_D=\{(F_{B1})_D\ (F_{B2})_D\ (F_{B3})_D\ (F_{B4})_D\}$, for the given features from the database, be two feature sets to be compared. Then, the mismatch measure $d_j(F_R, F_D)$ is defined as

$$d_j(F_R, F_D)=\frac{|(F_{Bj})_R-(F_{Bj})_D|}{1+|(F_{Bj})_R|-|(F_{Bj})_D|} \quad (5)$$

where, the denominator is used for feature magnitude normalization since the feature types are different in magnitude, and the value "1" is included to avoid a zero denominator value.

For the base-layer, if all the mismatch values are less than the pre-defined error values, two surfaces can be regarded as similar, and $d_j(F_R, F_D)=0$ when $F_R=F_D$. Here, even though the number of possible surface is one, the recognition procedure will be continued to the other layers to check whether the selected surface is the correct one or not. For the other layers, the mismatch measure values should be calculated for the six features, F_1-F_6. Thus, a total number of 16 features will be used to recognize the surface. The schematic diagram for the matching procedure is shown in Fig. 6.

5. Localization

The localization process is divided into two steps, rough and fine localization. In rough localization process, the location and orientation of the object are determined by analyzing the obtained database and the results from the image processing. However, since there still remain some localization errors due to the resolution of the vision system and other factors, one more step called the *fine localization* is employed to obtain more accurate results.

5.1 Rough localization

The area and position of the object can be determined from Eq. (A. 1) and (A. 2) respectively. Also, the orientation can be determined from the following equation.

$$\tan(2\theta)=\frac{2M_{11}}{M_{20}-M_{02}} \quad (6)$$

where, M_{pq} is the (p, q) central moment defined

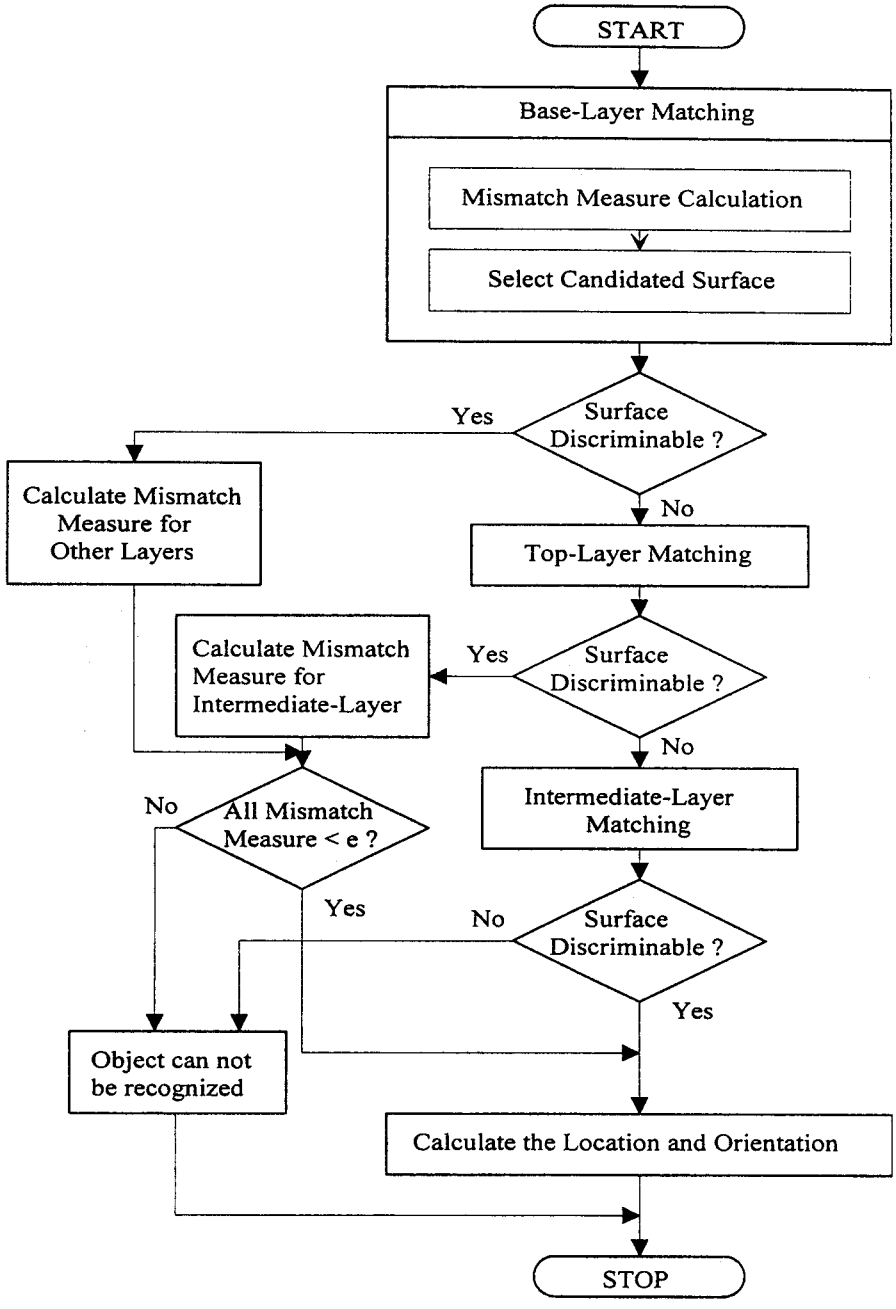

Fig. 6 Schematic diagram for matching and rough localization.

in Eq. (A. 4). However, the above equation can only give the orientation of the principal axes, thus, if the base-layer of the object has a rectangular shape, there are two possible cases. In this case, the exact orientation can be determined from the top-layer information as follows:

$$(\theta_w)_{CMM} = (F_{T7})_R - (F_{T7})_D \tag{7}$$

where $(\theta_w)_{CMM}$ is the orientation angle of the workpiece in the CMM coordinate.

Here, if the number of separate regions in the top-layer is larger than one, then the region that

has the longest distance from the base-layer centroid is taken to obtain a more accurate result.

5.2 Fine localization

The localization results based on the vision analysis can be affected by the lighting conditions, the resolution of the vision system, etc. Also, since the orientation of the object is determined by the difference in the inclinations of the top-layer in two different coordinate frames, the rough localization method may not give accurate results. Thus, in this study, the complex sculptured surface localization method proposed by Sahoo and Menq (1991) is used to determine the precise location of the object. However, since they determined the initial transformation amount by guessing, it may require a long iteration time. Thus, the rough localization results are used as initial values to reduce the calculation time. The basic idea of the minimization method is to find a transformation matrix by calculating the minimum distances between the discrete measured points and the given surface. For fine localization, several points on the surface will be digitized using the CMM, and numerical iteration methods can be used to minimize the distances. If the object on the CMM table is not at an exact position, then the coordinates of all its points on the surface will be changed. Therefore, by finding a transformation matrix that can minimize the sum of the distances, the coordinate transformation between the workpiece coordinate and the measurement frame can be determined.

5.2.1 Objective function formulation

When the object is not at an exact position on the CMM table, the measurement frame of the CMM should be transformed as

$$\{P_{wj}\}=\{P_{mj}\}[T_L] \tag{8}$$

where, $[T_L]$ is the transformation matrix that can minimize the distance errors, $\{p_{mj}\}$ is the measuring points specified in the measurement frame, and $\{p_{wj}\}$ is the transformed measuring points of the object.

To obtain the transformation matrix, Gunnarsson et al. (1987) and Sahoo et al. (1991) used different approaches. Gunnarsson et al. transformed the surface description in the CAD database, and Sahoo et al. used the inverse transformation of the measured points. In this study, the surface is transformed because it is easy to calculate the transformed surface descriptions. The transformed surface can be obtained by simply transforming the matrix that contains the control vertices coordinates as follows:

$$\bar{s}(u, v)=[U][M][P][M]^T[V]^T \tag{9}$$

and the transformed control vertices matrix $[P']$ can be given as

$$[P']=[T_L][P] \tag{10}$$

The objective function for the minimization method is to determine the variables in the transformation matrix by minimizing the distances between the measured points and the given surface. In general, the transformation matrix contains six transformation variables ($\theta, \Phi, \Psi, t_x, t_y, t_z$), where θ, Φ, Ψ are the rotation angles about the x-, y-, and z-axis, and t_x, t_y, t_z are the translational terms along the x-, y-, and z-axis, respectively. Therefore, the objective function can be formulated as

$$F(\phi, \phi, \psi, t_x, t_y, t_z)=\sum_{j=1}^{n} |\{p_{mj}\}-\{p_{sj}\}[T_L]|^2 \tag{11}$$

where $\{p_{mj}\}$ is the j^{th} measurement point, and $\{p_{sj}\}$ is the corresponding nearest point on the surface. $[T_L]$ is the transformation matrix to be determined which contains the six variables (ϕ, Φ, Ψ, t_x, t_y, t_z), and it has 4×4 form as follows:

$$[T_L]=\begin{bmatrix} c_2c_3 & s_1s_2c_3+c_1s_3 & -c_1s_2c_3+s_1s_3 & 0 \\ -c_2s_3 & -s_1s_2s_3+c_1c_3 & c_1s_2s_3+s_1c_3 & 0 \\ s_2 & -s_1c_2 & c_1c_2 & 0 \\ t_x & t_y & t_z & 1 \end{bmatrix} \tag{12}$$

where, $c_1=\cos\phi$, $c_2=\cos\varphi$, $c_3=\cos\Psi$, $s_1=\sin\phi$, $s_2=\sin\varphi$, $s_3=\sin\Psi$.

5.2.2 Minimization algorithms

To minimize the objective function given in Eq. (11), the partial derivatives of F with respect to all six transformation variables should be zero. Therefore, the following functions should be

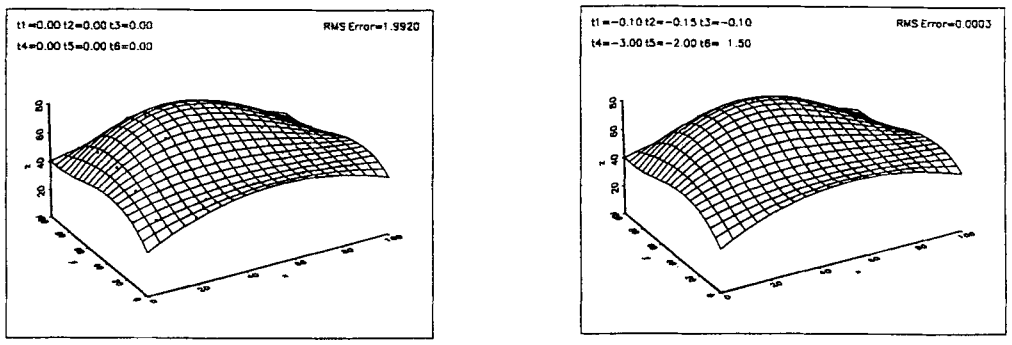

(a) Before fine localization (b) After fine localization

Fig. 7 Simulation result of the fine localization.

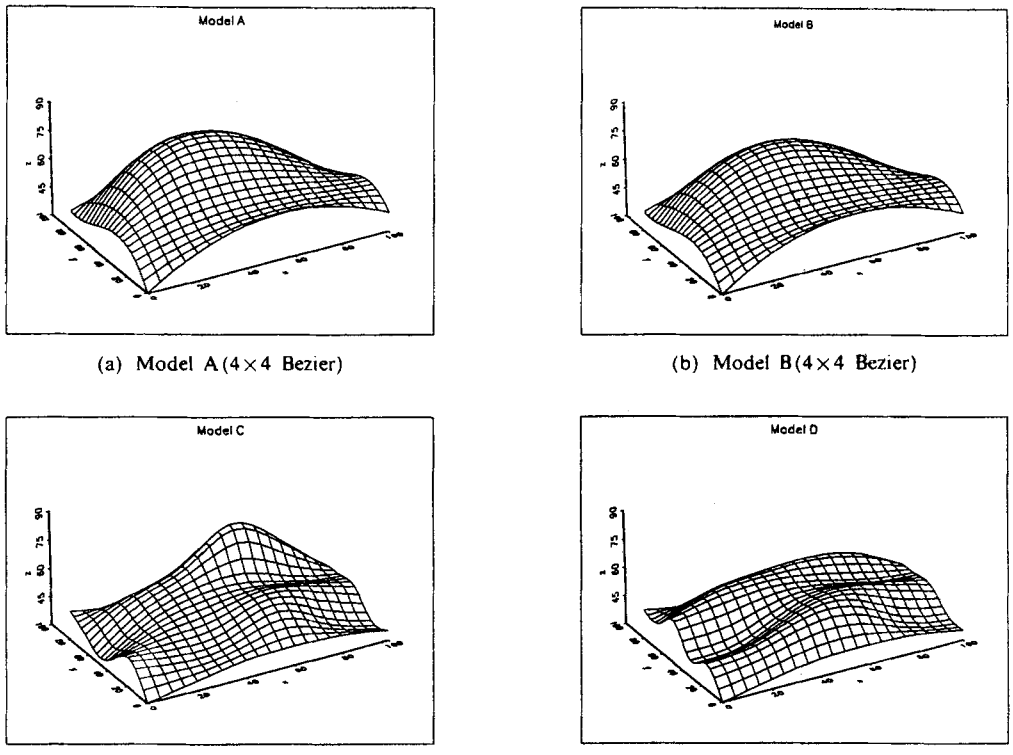

(a) Model A(4×4 Bezier) (b) Model B(4×4 Bezier)

(c) Model C(6×6 B-spline) (d) Model D(6×6 B-spline)

Fig. 8 Generated surfaces.

solved simultaneously.

$$f_i=\frac{\partial F}{\partial t_i}=0, \quad i=1, 2, \cdots, 6 \tag{13}$$

where $t_i=\theta$, ϕ, Ψ, t_x, t_y, t_z for $i=1$, 2, ..., 6, respectively.

The above equations can be solved by applying the conventional Newton-Raphson method. However, the function might diverge when the Newton-Raphson method is applied divectly since the global convergence properties of the method are poor. Therefore, in this study, a hybrid algorithm is used to solve the equations safely by combining the Newton-Raphson method and the Steepest Descent Method (Press et al., 1992). First, the Newton-Raphson method is applied to solve the equations, and whenever the solution is going out of bounds or the step size

is not being reduced rapidly enough, the steepest descent method is used. In this study, the results from the rough localization method are used as initial values to solve the numerical problem. Since these initial values are close to the final solution, the possibility of divergence by the Newton-Raphson method can be decreased significantly. The simulation result is shown in Fig. 7. From the Fig. 7(a) and (b), it can be known that the r.m.s. error is significantly decreased after transforming the surface according to the variables obtained from Eq. (13).

6. Experiment and Results

Following experiments are performed and the results are analyzed to verify the effectiveness of the proposed sculptured surface recognition/localization method.

6.1 Surface modeling and machining

In this study, four geometric databases are generated for the experiments. Two of the models, denoted by Model A and B, are generated using the Bezier surface generation method, and the others, denoted by Model C and D, are generated using the B-spline method. To show the effectiveness of the object recognition algorithm in the proposed system, all the workpiece models are designed to have the same base size of 100mm × 80mm. Generated surface models are shown in Fig. 8. Aluminum alloy blocks are machined using ball-end mills on the CNC vertical machining center to prepare the workpieces.

6.2 System set-up for the proposed method

For the experiments, two vision cameras (Allen-Bradley) are implemented on the CMM (Model Xcel, Brown and Sharpe). One camera is mounted on the ram of the CMM, and it is used to determine the location, orientation, and x, y-directional length of the surface by applying the binary image processing techniques. The other camera is installed at the side of the CMM, and it

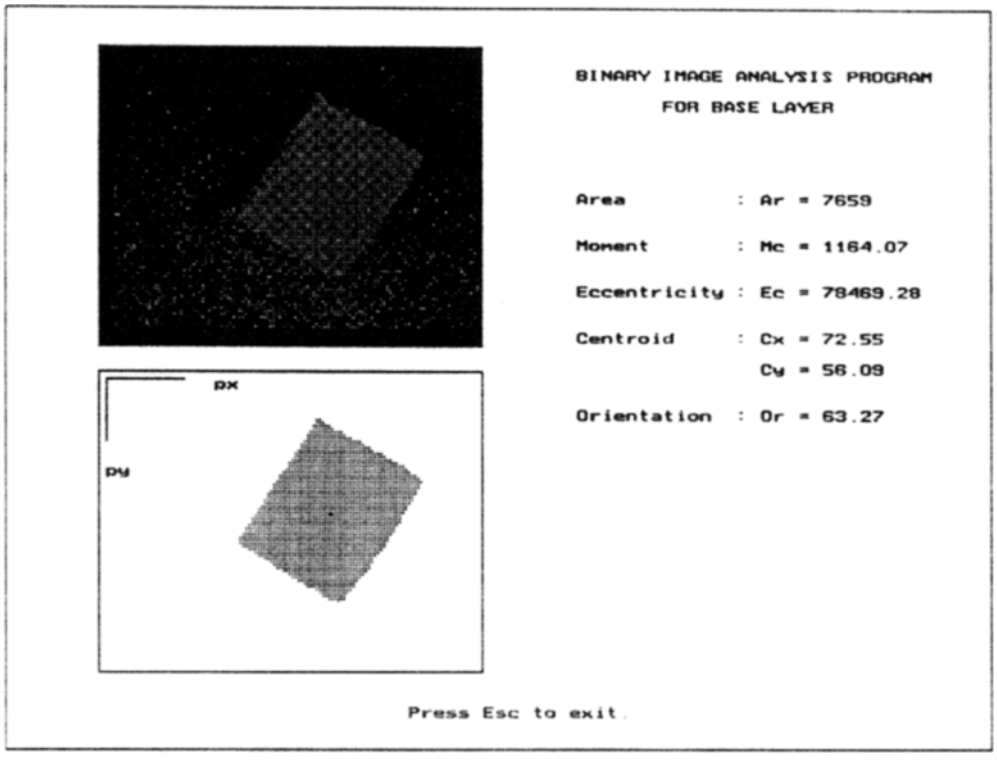

Fig. 9 Base-layer analysis using binary image processing.

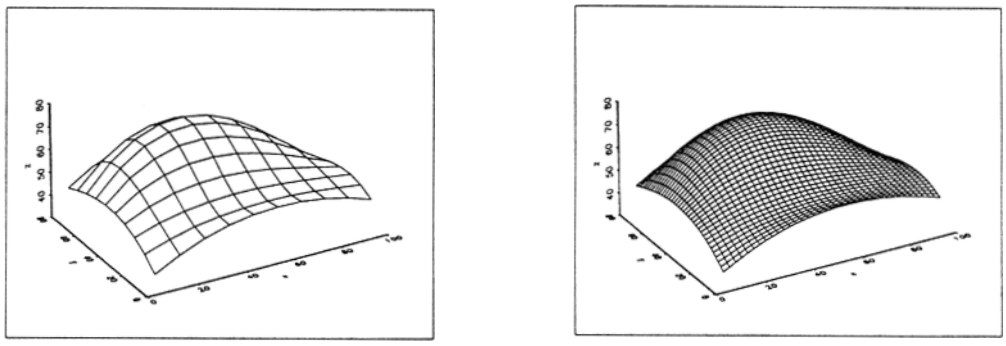

(a) Measured data (b) Surface by B-spline interpolation

Fig. 10 Surface construction using measured data.

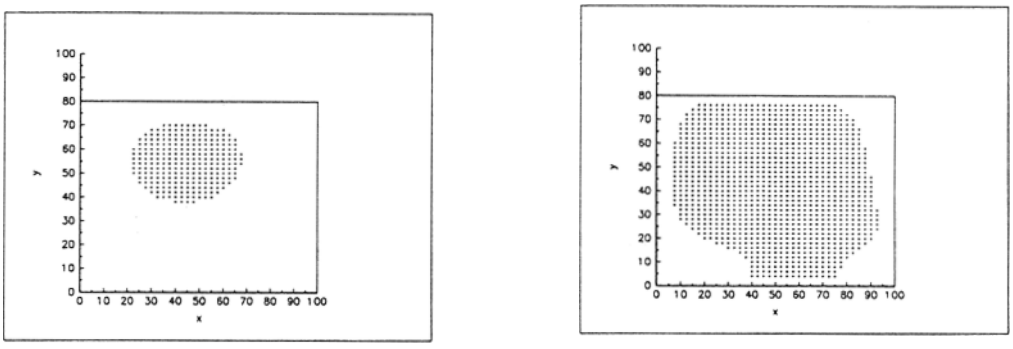

(a) Top-layer (b) Intermediate-layer

Fig. 11 Constructed Z-layers.

is used to determine the approximate maximum height of the surface. Imaging Technology's VISIONplus-AT OFG frame grabber is installed in the computer for image processing. A 512×512 pixel array is taken and compressed to a 128 128 pixel array, and required results are obtained using the implemented software from the compressed pixel array.

6.3 Recognition and localization

The properties of the base-layer are obtained by directly applying the binary image processing techniques to the image taken by the camera mounted on the CMM. The results are shown in Fig. 9. After determining the location, orientation, and the x, y-directional length of the surface using the binary image processing techniques, the CMM probe measures 10×10 points that are located at equal intervals in the xy-plane. The measured results and the B-spline interpolated surface are shown in Fig. 10(a) and (b) respectively, and the constructed Z-layers are plotted in Fig. 11. Then, the geometric properties of the constructed surface are compared with the given database, and the mismatch measure values are calculated for the recognition of the given surface. The results are shown in Table 2. From the table, it can be seen that all the mismatch measure values are within 10% error region. Thus, if the error region is set to 10%, the given set of surfaces can be recognized successfully. To apply the fine localization method, a 5×5 point array is extracted from the measured data since a 10×10 point array has already been measured for the construction of the object. The results from the image processing process are used as initial values for the fine localization. The results of the fine localization are shown in Table 3.

7. Conclusions

In this study, a sculptured surface recognition

Table 2 Mismatch measure values of the constructed surface.

Layer	Feature			Mismatch
		CAD Database	Constructed Database	Measure Values
Base-Layer	F_{B1}	8000.00	7659.00	0.022
	F_{B2}	71.60	71.15	0.003
	F_{B3}	1366.00	1164.07	0.080
	F_{B4}	90000.00	78469.28	0.068
Top-Layer	F_{T1}	1232.00	1440.00	0.078
	F_{T2}	64.44	64.04	0.003
	F_{T3}	207.33	217.02	0.023
	F_{T4}	4457.34	5137.84	0.071
	F_{T5}	1	1	0.000
	F_{T6}	15.32	16.51	0.037
Intermediate-Layer	F_{m1}	5648.00	6115.50	0.040
	F_{m2}	50.12	49.81	0.003
	F_{m3}	924.29	897.46	0.015
	F_{m4}	24132.50	28731.24	0.087
	F_{m5}	1	1	0.000
	F_{m6}	2.09	2.52	0.093

and localization method is proposed. As a first step, the sculptured surfaces are represented by the Z-Layer concept. By calculating the geometric properties of the Z-layers, required databases are obtained. To apply the Z-layer concept, the three-dimensional shape of the surface is constructed using the proposed vision guided CMM. Then, surface interpolation methods are applied to calculate the geometric properties of the constructed surface, and the best matching database is determined according to the calculated properties. Also, the location and orientation of the object can be easily determined by comparing the two databases. Next, the minimization algorithm is applied to obtain more accurate localization results. Finally, several experiments are performed to verify the proposed method, and the results show that the proposed method can be successfully implemented in real situation.

Table 3 Results of the fine localization.

Before	Variables	After
Φ	0.0	−1.583°
φ	0.0	−1.209°
Ψ	0.0	0.646°
t_x	0.0	−1.567mm
t_y	0.0	2.205mm
t_z	0.0	0.187mm
R.M.S. Error	0.755	0.043

References

Cho, M. W., Kim, M. K. and Kim, K., 1995, "Flexible Inspection System Based on a Vision Guided Coordinate Measuring Machine," *International Journal of Production Research*, Vol. 33, No. 5, pp. 1433~1448.

Gunnarsson, K. T. and Prinz, F. B., 1987, "CAD Model-Based Localization of Parts in Manufacturing," *Computer*, August , pp. 66~74.

Horn, B. K. P., 1986, *Robot Vision*, The MIT Press, Cambridge, Massachusetts.

Liu, C. and Tsai, W., 1990, "3D Curved Object Recognition from Multiple 2D Camera Views,", *Computer Vision, Graphics, and Image Processing*, Vol. 50, pp. 177~187.

Lo, C. and Don, H., 1989, "3-D Moment Forms: Their Construction and Application to Object Identification and Positioning," *IEEE Transactions on Pattern Analysis and Machine Intelligence*, Vol. 11, No. 10, pp. 1053~1064.

Mortenson, M. E., 1997, *Geometric Modeling*, John Wiley & Sons, New York, N. Y.

Press, W. H., Flannery, B. P., Teukolsky, S. A and Vettering, W. T., 1992, *Numerical Recipes in C*, Cambridge University Press, New York, N. Y.

Sahoo, K. C. and Menq, C., 1991, "Localization of 3-D Objects Having Complex Sculptured Surfaces Using Tactile Sensing and Surface Description," *ASME Journal of Engineering for Industry*, Vol. 113, pp. 85~92.

Sato, Y. and Honda, I., 1983, "Pseudodistance Measures for Recognition of Curved Objects," *IEEE Transactions on Pattern Analysis and Machine Intelligence*, Vol. PAMI-5, No. 4, pp. 362~373.

Takeuchi, Y., Shimizu, H. and Mukai, I., 1990,

"Automatic Measurement of 3-Dimensional Coordinate Measuring Machine by Means of CAD and Image Data," *Annals of the CIRP*, Vol. 39/1, pp. 565~568.

Wang, H. P., Hewgill, D. E. and Vickers, G. W., 1990, "An Efficient Algorithm for Generating B-Spline Interpolation Curves and Surfaces from B-Spline Approximations," *Communications in Applied Numerical Methods*, Vol. 6, pp. 395~400.

Wang, Y. F., Magee, M. J. and Aggarwal, J. K., 1984, "Matching Three-Dimensional Objects Using Silhouettes," *IEEE Transactions on Pattern Analysis and Machine Intelligence*, Vol. PAMI-6, No. 4, pp. 513~523.

Appendix: Geometric properties

Area

$$A_{obj}=\sum_{i=1}^{N_c}\sum_{j=1}^{N_r} b'_{ij} \quad \text{(A. 1)}$$

where b'_{ij} is the equivalent area of each pixel and N_r, N_c are the number of rows and columns of the array.

Centroid

The coordinate of the centroid (x_c, y_c) of the object can be as

$$x_c=\frac{m_{10}}{m_{00}},\quad y_c=\frac{m_{01}}{m_{00}} \quad \text{(A. 2)}$$

where the (p, q) moment of the object m_{pq} can be given as

$$m_{pq}=\sum_{i=1}^{N_c}\sum_{j=1}^{N_r} b'_{ij}(x'_i)^p(y'_j)^q \quad \text{(A. 3)}$$

Moment of inertia around the centroid

The (p, q) central moment of the image is defined as

$$M_{pq}=\sum_{i=1}^{N_c}\sum_{j=1}^{N_r} b'_{ij}(x'_i-y_c)^p(y'_j-y_c)^q \quad \text{(A. 4)}$$

Then, the moment of inertia of the image around the centroid m_{pq} can be given as

$$M_c=\frac{M_{20}+M_{02}}{M_{00}} \quad \text{(A. 5)}$$

Eccentricity

The eccentricity of the object can be calculated from the following equation.

$$E_c=\frac{(M_{02}-M_{20})^2+4M_{11}^2}{M_{00}^2} \quad \text{(A. 6)}$$

Distance between the centroids

$$d=[(x_{BC}-x_{LC})^2+(y_{BC}-y_{LC})^2]^{\frac{1}{2}} \quad \text{(A. 7)}$$

where (x_{BC}, y_{BC}) is the centroid of the base-layer, and (x_{LC}, y_{LC}) is the centroid of the other layers.

Inclination

$$\theta_r=\tan^{-1}\frac{y_{BC}-y_{LC}}{x_{BC}-x_{LC}} \quad \text{(A. 8)}$$